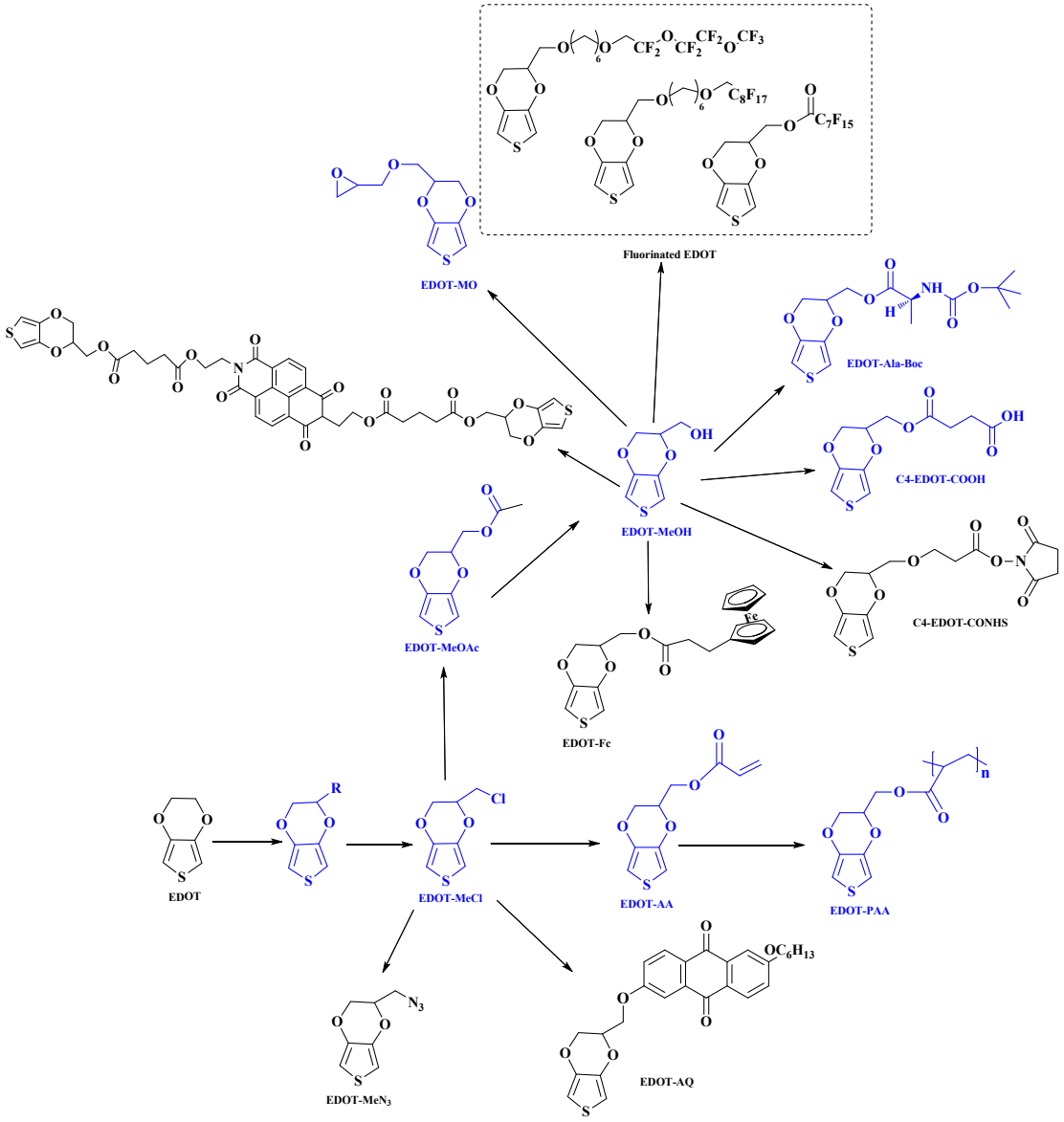

Scheme S1 Different EDOT derivatives in the recent literature. Our group also synthesized a variety of EDOT derivatives (blue structures).

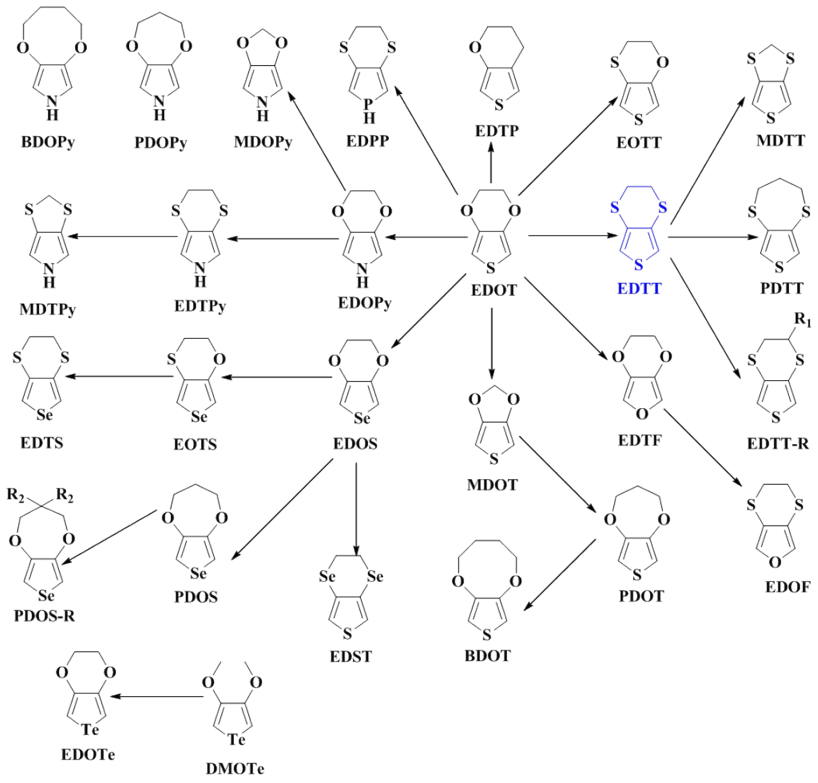

Scheme S2 Different EDOT analogs in the recent literature. An EDOT analog has been synthesized in our previous work (blue structure).

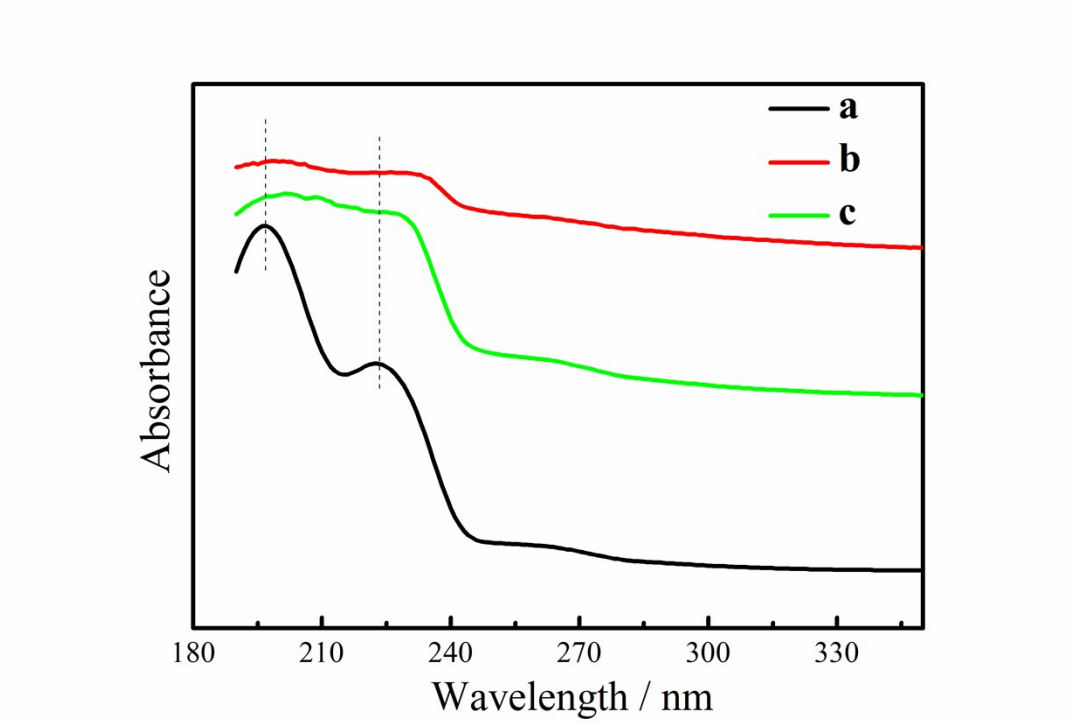

Figure S1 UV–vis spectra of poly(EDOT-*co*-EDOT-AA):PSS (a), poly(EDOT-*co*-EDOT-AA):PSS-GR (b), and poly(EDOT-*co*-EDOT-AA):PSS-HNPs-CMC (c).

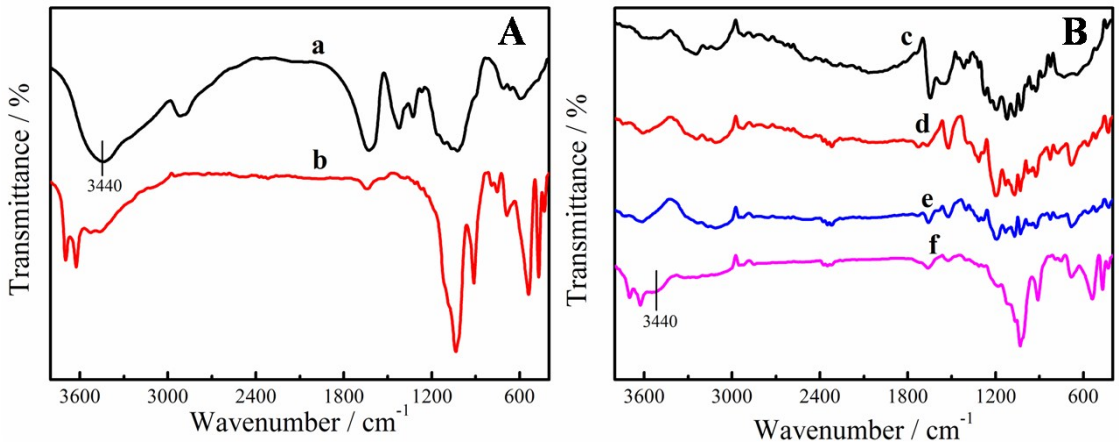

Figure S2 FTIR spectra of CMC (a), HNPs (b), GR (c), poly(EDOT-*co*-EDOT-AA):PSS (d), poly(EDOT-*co*-EDOT-AA):PSS-GR (e), and poly(EDOT-*co*-EDOT-AA):PSS-HNPs-CMC (f) in the range of 3800–400 cm^{-1}.

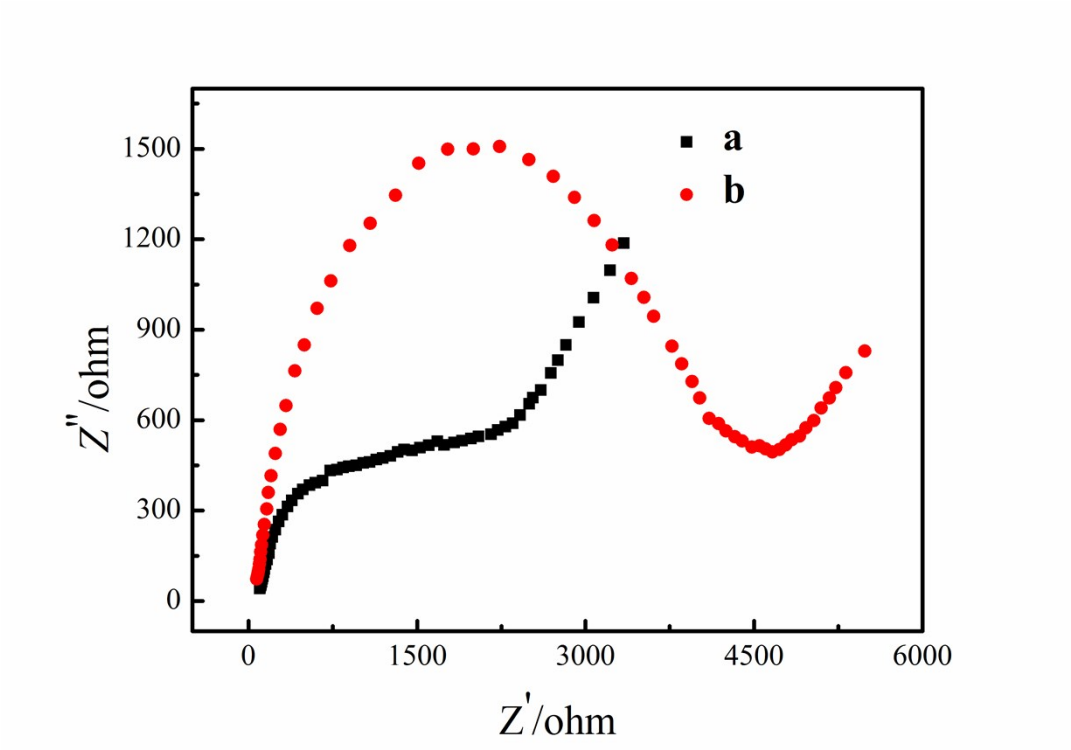

Figure S3 Nyquist plots of GR/GCE (a) and HNPs-CMC/GCE (b) electrodes in 10 mM $[Fe(CN)_6]^{4-/3-}$ solution containing 0.1 M KCl.

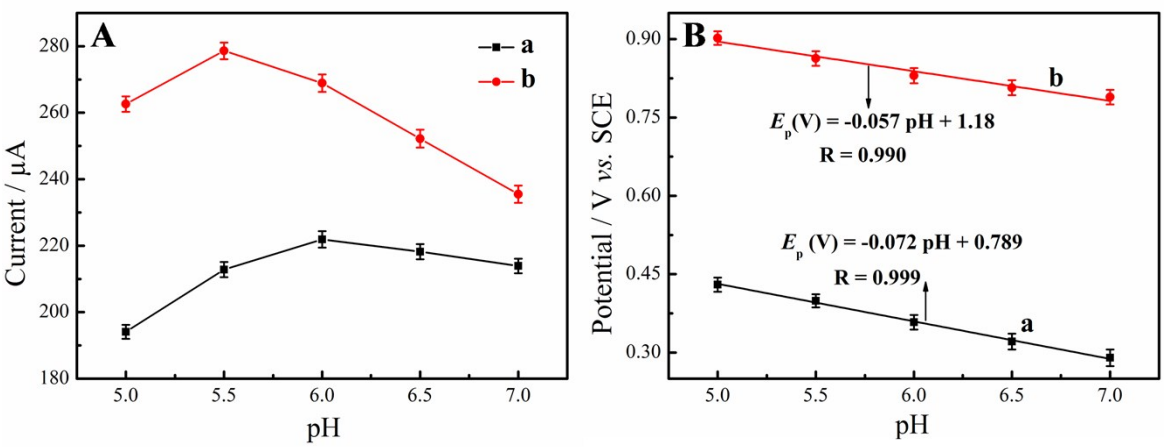

Figure S4 Effect of pH on the peak currents (A) and peak potentials (B) for the oxidation of 100 μM Ep (a) and 200 μM Trp (b) on poly(EDOT-*co*-EDOT-AA):PSS/GCE.

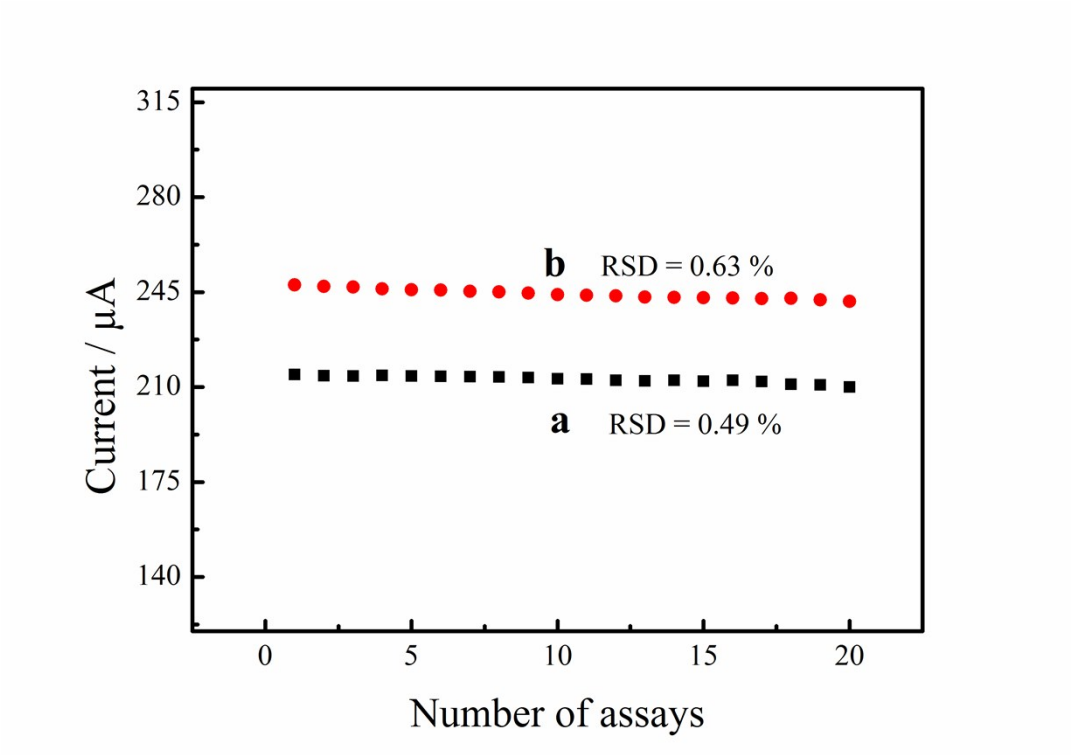

Figure S5 Operational stability for the electrochemical detection of both Ep and Trp of poly(EDOT-*co*-EDOT-AA):PSS/GCE.

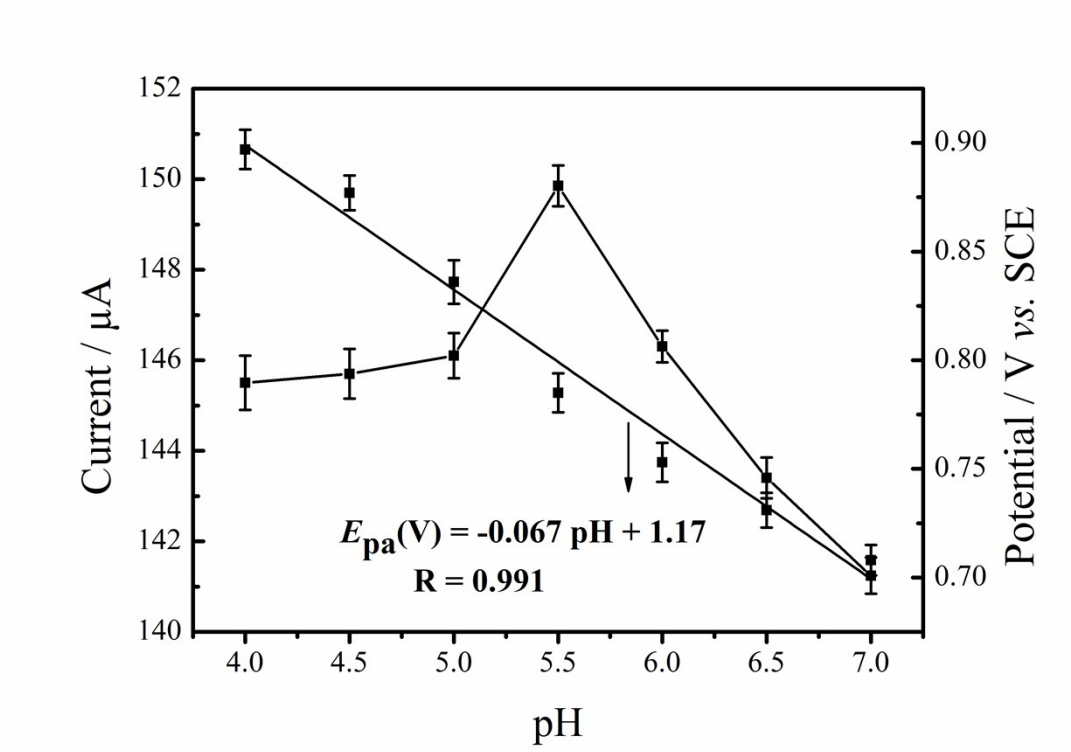

Figure S6 Effect of pH on the peak currents and peak potentials for the oxidation of 200 μM MH on poly(EDOT-*co*-EDOT-AA):PSS-GR/GCE.

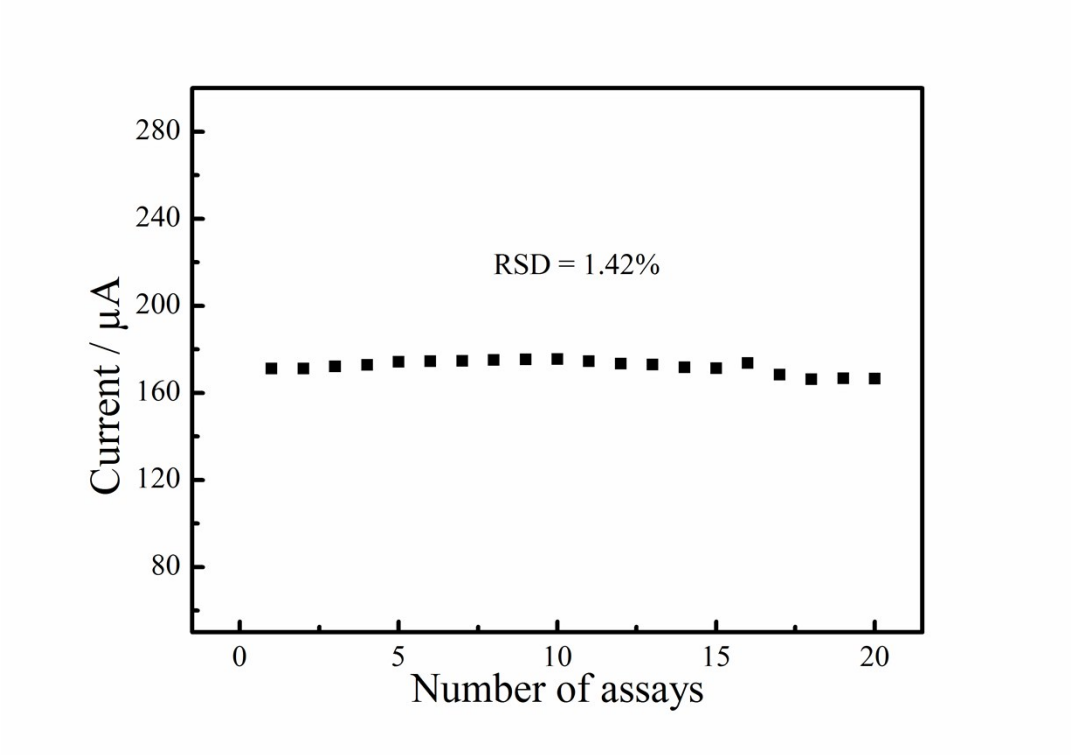

Figure S7 Operational stability for the electrochemical detection of MH of poly(EDOT-*co*-EDOT-AA):PSS-GR/GCE.

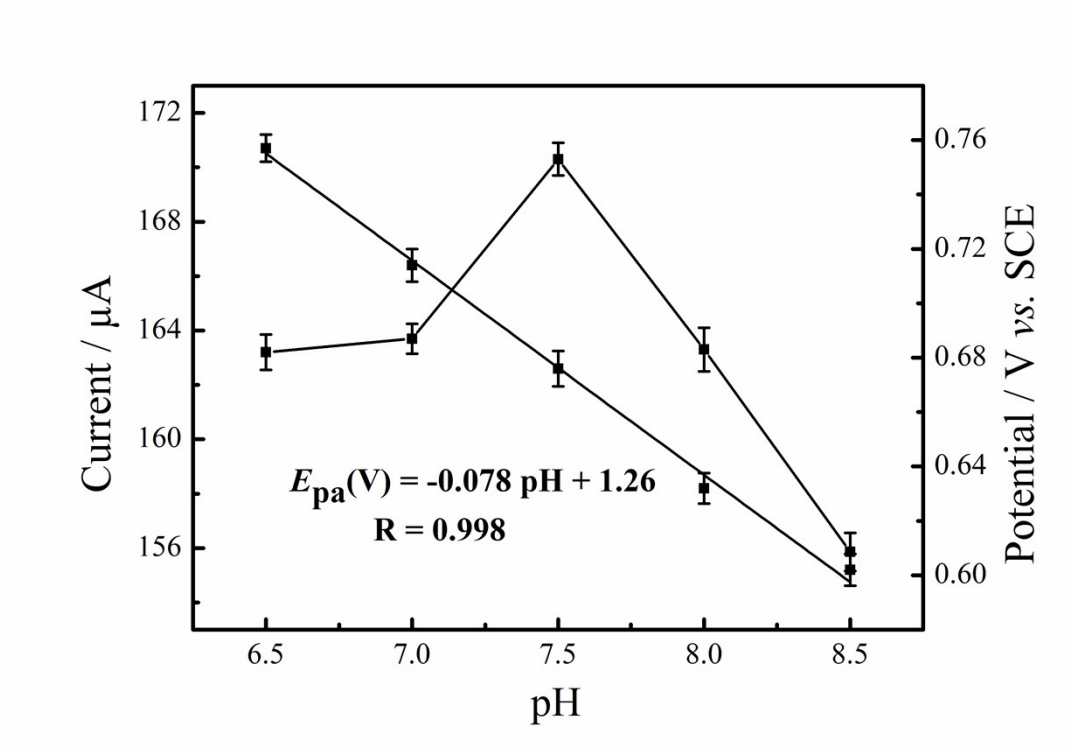

Figure S8 Effect of pH on the peak currents and peak potentials for the oxidation of 200 μM VB_6 on poly(EDOT-*co*-EDOT-AA):PSS-HNPs-CMC/GCE.

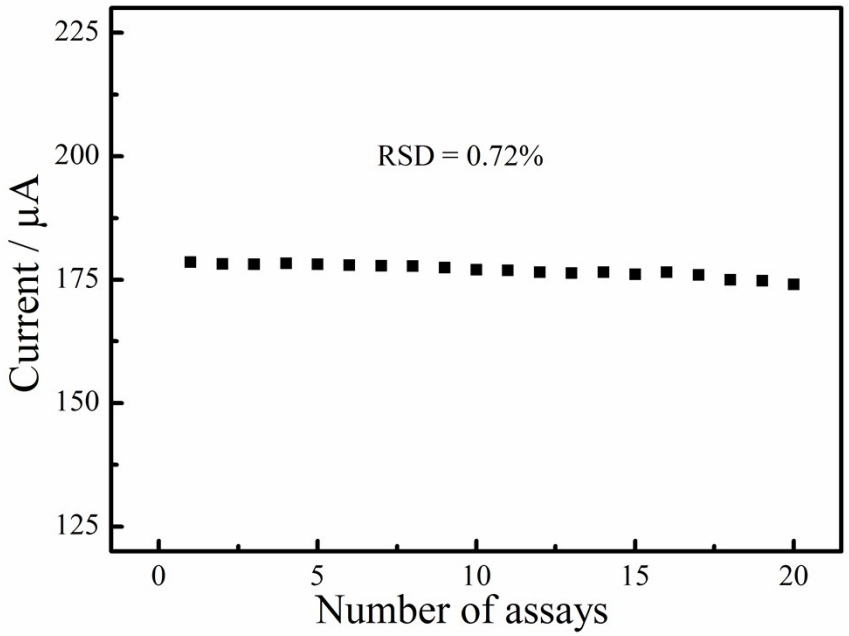

Figure S9 Operational stability for the electrochemical detection of VB_6 of poly(EDOT-*co*-EDOT-AA):PSS-HNPs-CMC/GCE.